Materials Research. 2013; 16(2): 392-403
DOI: 10.1590/S1516-14392012005000181

Statistic Evaluation of Cysteine and Allyl Alcohol as Additives for Cu-Zn Coatings from Citrate Baths

Julyana Ribeiro Garcia*[a], *Dalva Cristina Baptista do Lago*[a], *Fernando Lucas Gonçalves Silva*[a], *Eliane D'Elia*[b], *Aderval Severino Luna*[a], *Lilian Ferreira de Senna*[a]

[a]*Departamento de Química Analítica, Universidade do Estado do Rio de Janeiro – UERJ, Rua São Francisco Xavier, 524, Sala 427, Pavilhão Haroldo Lisboa da Cunha, Maracanã, CEP 20559-013, Rio de Janeiro, RJ, Brasil*
[b]*Departamento de Química Inorgânica, Universidade Federal do Rio de Janeiro – UFRJ, Av. Athos da Silveira Ramos, 149, Bloco A, Sala 634A, Ilha do Fundão, CEP 21941-909, Rio de Janeiro, RJ, Brasil*

Received: January 5, 2012; Revised: July 17, 2012

In the present work, cysteine and allyl alcohol were added to citrate baths as additives to Cu-Zn coatings on steel substrates. In order to verify the effects of the deposition parameters (current density, mechanical stirring speed, and additives) on the coating composition, electrochemical behavior, morphology, and microstructure properties of Cu-Zn coatings, the electrodeposition of the alloy was carried out using an experimental composite design 2^3, in which these parameters were considered the entry variables and the measured properties were the response variables. The confidence level was 95% and the results were shown as response surface diagrams. It was possible to verify that the current density affected the zinc content in the coating, while the coating produced from cysteine-contained bath presented the worse anticorrosive performance. In a general way, it was possible to observe that the studied parameters affected the morphology, grain size, and the electrochemical behavior of these coatings, although only a few response variables were statistically influenced by them.

Keywords: *electrodeposition, citrate bath, cysteine, allyl alcohol, Cu-Zn alloy*

1. Introduction

Alloy coatings can be obtained by electrodeposition, producing materials whose properties are dependent on the chemical composition of the deposited layers. However, each coating deposition system must be exhaustively studied before its commercially use because the simultaneous discharge of different ions on the cathode surface is a complex process that is influenced by several parameters, such as the substrate surface and the activity of each metallic ion on the double layer[1-4]. This last feature can influence the process to a great extent when the electrodeposition is performed with electrolytes that contain ligands and/or additives.

Additives (brightening and stress release compounds) are usually added to the electrodeposition bath to improve the properties of the coatings. These substances are generally organic compounds whose function is to refine the grains of the coatings, maintain the surface morphological components of the electrodeposits in the same plane, and produce coatings that reproduce the shine of the original metals[3,5]. The addition of these compounds causes a decrease in the internal stress release of the coating/substrate system, which generally favors the production of coatings without defects, pores or cracks. Therefore, coatings with improved shine, leveling, adherence, grain refinement, and appearance are obtained from baths containing additives.

*e-mail: lsenna@uerj.br

Amino acids can be applied as additives for electroplating. The interaction of these compounds with metal surfaces may occur via either the amino or carboxylate groups, depending on the conditions of interaction and the substrate[6]. In an electrodeposition process, amino acids can act as ligands for metallic ions; they can also enhance or decrease the intensity of parallel reactions (for example, the hydrogen evolution reaction, HER)[7,8]. The side chain of the amino acid can also play an important role. For example, with a sulfur-containing amino acid like cysteine ($HS–CH_2–CH(NH_2)–COOH$), the strong affinity of sulfur for different metals is a key factor[9]. Cysteine presents a thiol or sulfhydryl (S–H) group that is the most chemically reactive site on a protein under physiological conditions[10]; it is also a preferred ligand for the metallic cations. However, these thiol groups may suffer oxidation, causing the dimerization of the cysteine molecule. Cysteine can also adsorb onto the surfaces of different metals, which has been reported in the literature using several surface science and electrochemical techniques[6].

Allyl alcohol is a leveling agent additive that can also be added to an electroplating bath to increase the brightening of the produced coatings. However, few data are available in the literature concerning the role of this additive on the electrodeposition process. It is probable that its metallic complexes must be linked by the allyl radical, mainly in an acidic medium. Vagarlyuk et al.[11,12] indicated that a copper (I)-allyl alcohol complex may exist in an acidic medium.

Senna et al.[13] suggested that the presence of allyl alcohol in a Cu-Zn pyrophosphate bath could decrease copper activity in the solution as a result of the formation of a new and more stable Cu-complex, in which allyl alcohol and pyrophosphate ions would act as a mixed ligand. Such additive complex formed with the metal ions may increase their adsorption at the electrode surface, thus increasing their reduction rate (induced adsorption)[5]. In addition, its stress relieving properties may also prevent coating embitterment caused by the simultaneous HER, producing refined compact grains and bright Cu-Zn coatings[14]. Lustrous coatings were also obtained in the presence of allyl alcohol in certain modes of electrolysis and under stirring when Sn coatings were produced from a complex bath[15].

Previously, we have shown that sodium citrate can produce adherent and corrosion resistant Cu-Zn alloys[16]. However, only a few coatings presented a lustrous appearance. In the present work, a 2^3 composite design was used to verify the influence of the addition of additives (cysteine and allyl alcohol) to the base citrate bath, the applied current density (***I***), and the mechanical stirring speed (***S***) on the metal content of the alloy (***%m/m Cu*** and ***%m/m Zn***), the corrosion current density (I_{corr}), the microstructure, and the morphology of the Cu-Zn alloys produced on mild steel AISI 1020.

2. Experimental Procedures

2.1. *Cathodic polarization curves*

Galvanostatic polarization curves were obtained at 25 °C for current densities between 0.1 and 120 A m^{-2} using a potentiostat/galvanostat developed for this purpose[16]. The mechanical stirring speed was varied from 0 to 400 rpm. The experiments were performed in the baths presented in Table 1. All chemicals used were pure grade. A three-electrode system was applied in which the working electrode was a mild steel AISI 1020 disk with 4.9×10^{-4} m^2 of area, previously polished with sand paper and degreased with sodium lauril sulfate solution, while the counter electrode was a brass slab (67% m/m Cu and 33% m/m Zn). The potential was measured versus a saturated sulfate reference electrode (SSE).

2.2. *Electrodeposition experiments*

To verify the best conditions for the production of a coating/substrate system with elevated corrosion resistance, the Cu-Zn alloy electrodeposition was performed by employing a 2^3 composite design. The influence of the electrodeposition parameters (independent variables) composition bath (***B***), applied current density (***I***), and mechanical stirring speed (***S***), on the process responses, which included the content of the metals in the alloy (***%m/m Cu*** and ***%m/m Zn***), corrosion current density (I_{corr}), microstructure, and morphology of the Cu-Zn alloys produced on AISI 1020 mild steel, were then evaluated based on the design matrix shown in Table 2. The same table also presents the codified and real values for the independent variables. The ***I*** and ***S*** values were chosen from the cathodic polarization curves and the earlier results[17]. The Cu-Zn coatings were obtained using the same apparatus and the same three-electrode cell mentioned previously. A commercial software package (STATISTICA for Windows, release 7.0) was used for the experimental data regression analysis.

2.3. *Coating characterization*

2.3.1. Chemical analysis

Flame atomic absorption spectrometry (*Perkin-Elmer AAnalyst 300*) was used to determine the content of copper and zinc in the alloy coatings produced from the baths shown in Table 1 after the dissolution of the coatings in HNO_3 20% v/v.

Table 1. Chemical composition and pH values of the studied electrolytes.

Bath	Chemical composition (mol L^{-1})					pH
	$CuSO_4.7H_2O$	$ZnSO_4.5H_2O$	$Na_3C_5H_6O_7$	Cysteine	Allyl alcohol	
1	0.02	0.20	1.00	-	-	6.59
2	0.02	0.20	1.00	0.001	-	6.77
3	0.02	0.20	1.00	-	0.07	6.12

Table 2. Composite design 2^3 experimental matrix, showing codified and normal values of the studied variables.

Run no.	Current density (cod.)	Mechanical stirring speed (cod.)	Bath composition (cod)	Current density (A m^{-2})	Mechanical stirring speed (rpm)	Bath composition*
1	–1	–1	–1	15	300	BB
2	+1	–1	–1	20	300	BB
3	–1	+1	–1	15	400	BB
4	+1	+1	–1	20	400	BB
5	–1	–1	+1	15	300	BA
6	+1	–1	+1	20	300	BA
7	–1	+1	+1	15	400	BA
8	+1	+1	+1	20	400	BA

*BB = Base Bath (Bath 1 from Table 1); BA = Bath containing additives (Baths 2 and 3 from Table 1).

2.3.2. Electrochemical analysis

The coating/substrate systems obtained from the solutions shown in Table 1 were electrochemically evaluated by their potentiostatic polarization curves performed with a potentiostat/galvanostat PG29 (*Omnimetra Instruments*). The potential was varied from –1 to +1 V_{SCE} at a scan rate of 5 mV s^{-1}. The experiments were performed in a 0.5 mol L^{-1} NaCl solution (pH = 6.5) at 25 °C. The counter electrode was a platinum net, and the reference electrode was saturated calomel (SCE). $\boldsymbol{I_{corr}}$ was obtained from the Tafel slopes of the polarization curves.

2.3.3. Morphological characterization

The morphologies of the coatings were evaluated using a scanning electron microscope (*JEOL JSM 6460LV*). The coatings were ultrasonically cleaned for 15 minutes, dried and attached to the stub with conductive tape. The analyses were conducted in high vacuum using the secondary electron mode.

2.3.4. Microstructure characterization

X-rays diffractograms of the coatings were obtained using a diffractometer (*Siemens D-6000*) with a copper source (CuKα = 1.5406 Å). The 2θ range extended from 10° to 90°, which was scanned at a rate of 0.020° s^{-1}. The more prominent diffractogram lines from the Cu-Zn alloy deposit were fitted by a Gaussian equation (using Microcal Origin®, release 8.0), and the values of 2θ obtained were used to calculate the *d* (h k l) values of the diffraction lines. The phase identification was conducted using JCPDS-PDF standard data[18]. The full width at half maximum (***FWHM***), estimated grain size ($\boldsymbol{G_S}$), and height of the diffraction lines (***H***) of the most intense diffraction line (100%) were also evaluated. The grain size was related to the particle diameter using Equation 1[19]:

$$d_P = \frac{k\lambda}{\beta \cos\theta} \quad (1)$$

where d_p is the particle diameter (Å), k is a constant related to the crystal microstructure, λ is the wavelength of the incident radiation (Å), and β is the enlargement of the diffraction line, which can be calculated from Equation 2[19]:

$$\beta = \sqrt{B_M^2 - B_S^2} \quad (2)$$

where B_M is the measured ***FWHM*** value and B_S is the ***FWHM*** of a standard material.

3. Results and Discussion

3.1. *Cathodic polarization curves*

The polarization curves were used to select the current density values used for the electrodeposition experiments and to verify if this technique is able to show the effects of the additives on the Cu-Zn electrodeposition process. Figures 1a, b present the polarization curves for steel substrates immersed, respectively, in Baths 2 and 3 of Table 1, at stirring speeds (***S***) ranging from 0 to 400 rpm. In all cases, substrate depolarization was observed as ***S*** increased. Strong polarization had been noted for the deposition of copper and copper alloys in a citrate electrolyte without stirring because of the effects of blocking species (mainly Cu-citrate complexes)[14,18-20]. This influence usually decreased at higher values of ***S***[14,15,18] due to the increase in the mass transport. This effect was less pronounced for the curves of Bath 2 (Figure 1a), for which cysteine was added to the citrate bath. Cysteine can also be adsorbed to the substrate surface, and it could have probably acted as another blocking species at low ***S*** values.

To avoid any kind of blocking effect, the polarization curves of the substrates immersed in the baths of Table 1 at 300 and 400 rpm were compared (Figure 2) to verify the influence of low amounts of cysteine and allyl alcohol added to Bath 1, which contains only Cu (II), Zn(II) and citrate ions. There was no difference among the polarization curves, independent of the ***S*** and bath ***B*** used. Because cysteine increases the overpotential for HER, zinc deposition was expected to take place at less negative potentials. However,

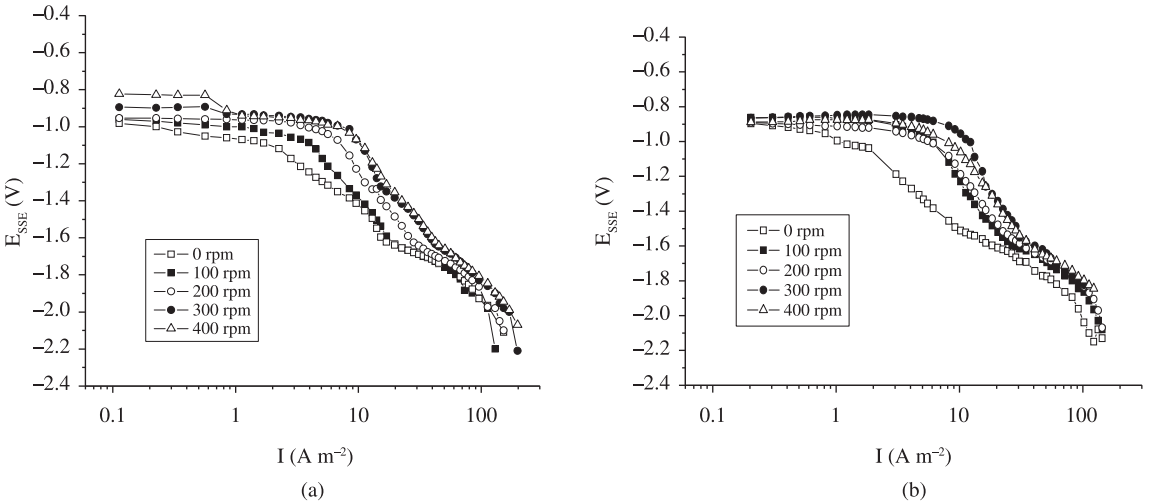

Figure 1. Cathodic polarization curves of carbon steel AISI 1020 in Baths 2 and 3 of Table 1, using mechanical stirring speeds ranging from 0 to 400 rpm.

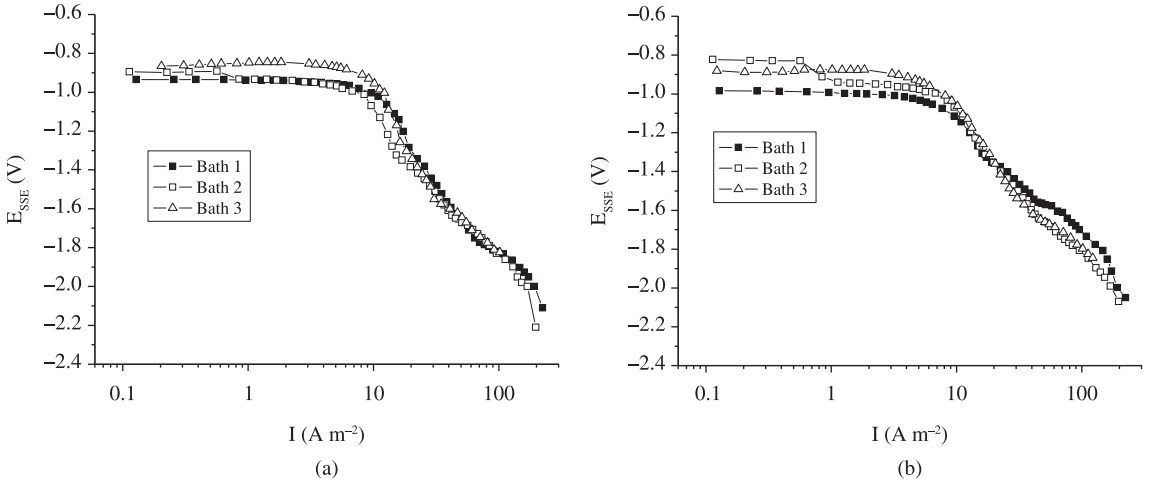

Figure 2. Cathodic polarization curves of carbon steel AISI 1020 in the baths of Table 1 at a) 300 rpm and b) 400 rpm.

this effect was not observed with the applied electrochemical technique. Additionally, the influence of allyl alcohol as a surface leveling agent in the reduction process of Cu-Zn alloys could not be verified by the curves of Figure 2. These results show the limitations of the applied technique for the description of the effects of the mentioned variables on the electrodeposition process. This desired result can be probably achieved by the electrodeposition experiments, as shown below.

Based on these results and the earlier ones published by Senna et al.[13] and Ferreira et al.[16], two ***I*** and two ***S*** levels were selected (Table 2) for the electrodeposition experiments.

3.2. *Electrodeposition experiments*

The surface model obtained from the relationship between the responses and the varied parameters of the electrodeposition process using a 2^3 composite design is represented by Equation 3.

$$\hat{y} = b_0 + b_1x_1 + b_2x_2 + b_3x_3 + b_{12}x_1x_2 + b_{13}x_1x_3 + b_{23}x_2x_3 + b_{123}x_1x_2x_3 \quad (3)$$

where $\hat{y}$ is the studied response variable (***%m/m Cu***, ***%m/m Zn***, $\boldsymbol{I_{corr}}$, ***2θ***, ***FWHM***, and ***H***); x_1, x_2, and x_3 correspond to the electrodeposition parameters ***I***, ***S***, and ***B***, respectively; x_ix_j represents the interaction between two of the parameters; and $x_ix_jx_k$ is the interaction among the three parameters. This equation was applied to all variables based on the *t* test, and only the effects that present significant influence ($p < 0.05$) will be shown. It is important to point out that even though some individuals trends could be observed in how ***I***, ***S***, and ***B*** influenced the response variables, the final results concerning the influence of the studied parameters were obtained using the response surfaces, which take in account all the responses observed for each effect. These surface responses are represented as three-dimensional diagrams, in which the entry variables (studied electrodeposition parameters) are presented in their codified values (Table 2) in the x and y axes, while the response variables (***%m/m Cu***, ***%m/m Zn***, $\boldsymbol{I_{corr}}$, ***2θ***, ***FWHM***, and ***H***) are presented in the z axis, with their real values[21].

In all cases, the particular bath used is a qualitative parameter that is only considered to be –1 (base bath) or +1 (bath with additives) in the following results. Therefore, this parameter cannot assume any other values because other values would not have a physical meaning. All of the numerical results obtained with this model are shown in Table 3.

3.3. *Copper content in the coating (% m/m Cu)*

Table 3 presents the ***% m/m Cu*** results for the coatings produced with the baths shown in Table 1. The values of ***% m/m Cu*** in the coatings vary from approximately 63% m/m (for Bath 2 at 20 A m^{-2} and 400 rpm) to 99% m/m (also for Bath 2, at 15 A m^{-2} and 300 rpm). Therefore, different deposition conditions seem to influence the copper concentration, producing coatings that can be rich or poor in copper.

Based on the composite design described in Table 2, only the average coefficient (b_0) showed significant statistic meaning concerning the influence of the deposition parameters on the ***% m/m Cu*** values, at a confidence level of 95%. This result is shown in Equations 4 and 5 for Baths 2 and 3, respectively. Although the adjusted R^2 was low in both cases (approximately 65%), Figure 3 still shows the main effects (in this case, only b_0) of the presence of cysteine and allyl alcohol on the studied parameters in the base citrate bath.

$$\%Cu(\hat{m}/m) = 83 \quad (4)$$

$$\%Cu(\hat{m}/m) = 82 \quad (5)$$

Ferreira et al.[16] observed an elevation in the ***% m/m Cu*** values with increasing ***S*** and decreasing ***I*** for the base citrate bath (Bath 1). This behavior was related to the following two properties of the system: first, copper is easily reduced mainly at low values of the current density (where other parallel reduction reactions, such as Zn ion reduction and HER, cannot compete with this main reaction); second, ion transport is favored by ***S***, thus increasing the Cu content in the coating. Additionally, when pH variation and citrate concentration are considered, the proposed mechanisms for

Table 3. Numerical results obtained with the proposed composite design 2^3; B1 – results obtained using Bath 1; B2 – results obtained using Bath 2; B3 – results obtained using Bath 3.

Run No.	Current density (cod.)	Mechanical stirring speed (cod.)	Bath composition (cod)	Cu content (% m/m)	Zn content (% m/m)	I_{corr} (A m^{-2})	FWHM	G_s (Å)	H (a.u.)
1(B1)	–1	–1	–1	91.15	13.85	0.04	0.44	19.2	156.2
2(B1)	+1	–1	–1	67.47	17.25	0.06	0.54	15.6	178.8
3(B1)	–1	+1	–1	91.50	7.89	0.10	0.87	9.7	85.7
4(B1)	+1	+1	–1	88.07	17.49	0.12	0.88	9.6	98.0
5 (B2)	–1	–1	+1	99.00	1.03	0.30	1.34	6.2	19.5
6 (B2)	+1	–1	+1	79.71	10.54	0.30	0.38	22.2	188.6
7 (B2)	- 1	+1	+1	83.30	0.63	0.25	1.22	6.9	48.2
8 (B2)	+1	+1	+1	63.35	3.73	0.20	0.41	20.9	172.7
9 (B3)	–1	–1	+1	81.56	8.71	0.08	0.44	19.2	156.0
10 (B3)	+1	–1	+1	71.60	17.77	0.15	0.86	9.8	83.8
11 (B3)	–1	+1	+1	92.89	5.27	0.18	0.84	10.0	71.9
12 (B3)	+1	+1	+1	72.64	17.81	0.18	0.92	9.2	64.4

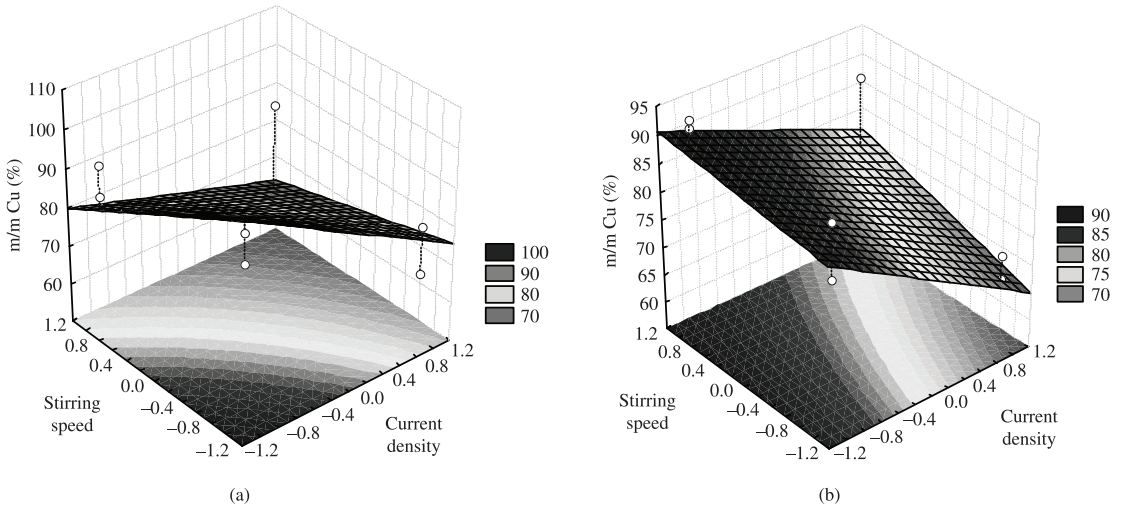

Figure 3. Fitted response surface of standardized effects of ***I*** and ***S*** for ***% m/m Cu***: a) Bath 2; b) Bath 3.

Cu deposition in a citrate medium[22,23] established that several Cu-citrate complexes are directly reduced without previous dissociation. After reduction, the resulting species can be either directly incorporated into the deposit or undergo decomplexation, yielding molecules of free complexing agents. Therefore, an increase in ***S*** can also enhance the transport of any free ligand from the electrode surface to the solution bulk after discharge.

Concerning the coatings produced from Bath 2, which contains cysteine, Figure 3a shows that an increase in ***% m/m Cu*** tends to occurs at small values of both ***I*** and ***S***. The cause of the ***I*** influence can be considered to be similar to what has been observed by Ferreira et al.[16] for Bath 1. In fact, Silva et al.[17] have shown that, for the smallest ***I*** value used, the substrate potential for the deposition of Cu-Zn alloy from a citrate bath containing cysteine was shifted to more positive values when compared to that obtained from the base citrate bath, enhancing the copper content in the coating. However, the ***S*** effect was in an opposite direction to what was projected. As cysteine can adsorb on the copper surface[6], it would be expected that a decrease in ***S*** should facilitate this adsorption, increasing the polarization and making the deposition of copper more difficult. In Bath 2, the bulk electrolytic solution is at pH = 6.77, which is higher than the first pK_a of cysteine (pK_{a1CYS} = 1.71) and smaller than its second pK_a (pK_{a2CYS} = 8.33), suggesting that the possible ionic forms of cysteine in solution at this pH range were NH_3^+/SH/COO^- (zwitterionic form) and NH_2/SH/COO^- (basic form)[6]. It is known, however, that the pH in the substrate/solution interface may increase due to the HER reduction[13,14], which can favor the presence of the basic form of cysteine. Using infrared analysis to study the adsorption of cysteine on copper surface, Marti et al.[6] have shown that, at intermediate values of pH, there was a higher fraction of NH_2 groups adsorbed, which was reflected by the intense signal at 1080 cm^{-1}. Additionally, Sukava et al.[24] have shown that the adsorption of cysteine onto copper electrodes during copper electrodeposition was sufficiently dynamic and the adsorbate phase was sufficiently mobile to enable the copper lattice to grow without covering the additive

molecules. Therefore, the adsorption of cysteine on the basic form might have been favored at the present experimental conditions, probably changing the cathodic processes kinetic and enhancing the copper reduction, resulting in a higher copper content in the coating.

Similar to the observations of Ferreira et al.[16] for the base-citrate bath, an increase in ***% m/m Cu*** tends to occur at small values of ***I*** for the coatings produced from Bath 3, which contains AA (Figure 3b). This behavior was observed for all ***S*** values, although a small increase in ***% m/m Cu*** was noted for high ***S*** values. Allyl alcohol can act as a ligand for Cu (I) in acidic media[12]. Moreover, because this additive is a leveling agent, it was expected that its adsorption on the substrate surface could affect the copper deposition process. An increase in ***S*** may remove the additive, as well as any blocking agent, from the substrate surface, enhancing copper deposition. Nonetheless, under the conditions of this study, the effect of ***S*** was more pronounced for the bath without allyl alcohol.

3.4. *Zinc Content in the coating (**% m/m Zn**)*

The ***% m/m Zn*** results for the coatings produced with the baths shown in Table 1 are also presented in Table 3. The smallest values of ***% m/m Zn*** were observed in the coatings produced from Bath 2, which indicates that the presence of cysteine might have affected this variable. This result could be related to the stability of copper and zinc complexes with citrate and to the formation of a stable zinc-cysteine complex[25,26]. The stability constants for Cu-Citrate and Zn-Citrate complexes are 1.62×10^{14} and 4.45×10^{7}, respectively[25]. It means that in a base citrate bath, all Cu (II) ions are complexed with citrate and most of the Zn (II) ions are not complexed with this ligand. The stability constant for the zinc-cysteine complex is 9.33×10^{8}, when small amounts of cysteine are present in the bath[26] (as in Bath 2), which is almost the same order of magnitude of the Zn-Citrate constant. It suggests that part of the Zn (II) ions may also be complexed with cysteine, which could interfere in their deposition process. However, it is important to point out that the influences of the deposition parameters on the ***% m/m Zn*** values of coatings obtained from Bath 2 were not statistically significant, at a confidence level of 95%. Therefore, further experiments are still needed to reach a final conclusion on this topic.

On the other hand, for coatings produced from Bath 3, only the ***I*** parameter affected the ***% m/m Zn*** values significantly, as shown in Equation 6. This result means that high values of ***I*** enhance the ***% m/m Zn*** in the coatings. Because this effect has also been verified for coatings produced from citrate baths without additives[16], the presence of allyl alcohol in the bath cannot be said to influence the ***% m/m Zn*** values significantly, as observed in Table 3. The adjusted R^2 was above 95% in this case.

$$\%Zn(\hat{m}/m) = 13 + 4.3I \quad (6)$$

Figure 4 presents the surface responses showing the effects of the studied deposition parameters on the ***% m/m Zn*** values. As no statistical influences on the studied variables were observed for the coatings of Bath 2, only the trends verified for the coatings produced from Bath 3 are shown. As a comparison, it is interesting to know that, for the coatings produced in the base citrate bath, the ***% m/m Zn*** values increased in opposition to the increasing ***% m/m Cu*** values[16]; that is, ***% m/m Zn*** increased for increasing ***I*** and decreasing ***S***. Large current densities are needed to promote the reduction of zinc ions to metallic zinc. On the other hand, forced convection may improve copper deposition and decrease the zinc content in the coating, as observed earlier. In agreement with Equation 6, Figure 4 shows that an increase in ***% m/m Zn*** can be obtained at higher values of ***I***, regardless of the ***S*** value used.

3.5. *Coating characterization*

3.5.1. *Corrosion current density (**I_{corr}**)*

The produced coatings were electrochemically evaluated by their polarization curves in a 0.5 mol L^{-1} NaCl solution. Figure 5 present an example of these curves, obtained from the coatings produced at 15 A m^{-2} and 300 rpm. There were almost no differences among the curves obtained for coatings produced from the same baths, at other deposition conditions. The steel substrate was submitted to the same

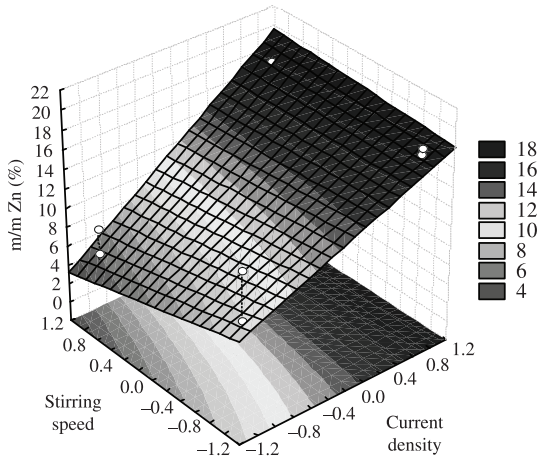

Figure 4. Fitted response surface of standardized effects of ***I*** and ***S*** for ***% m/m Zn***: Bath 3.

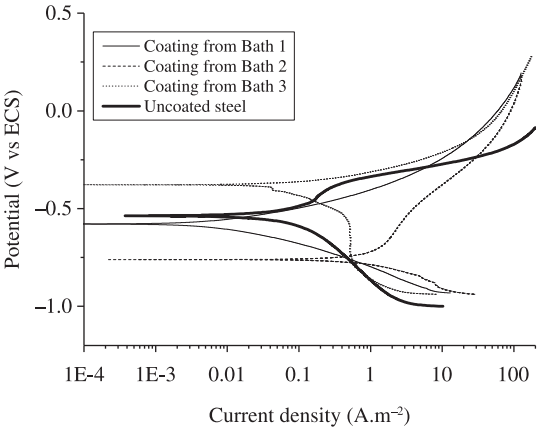

Figure 5. Polarization curves of the coated substrates produced from the baths of Table 1 in NaCl 0.5 mol L^{-1}. Polarization curves of uncoated substrate is also shown, as comparison.

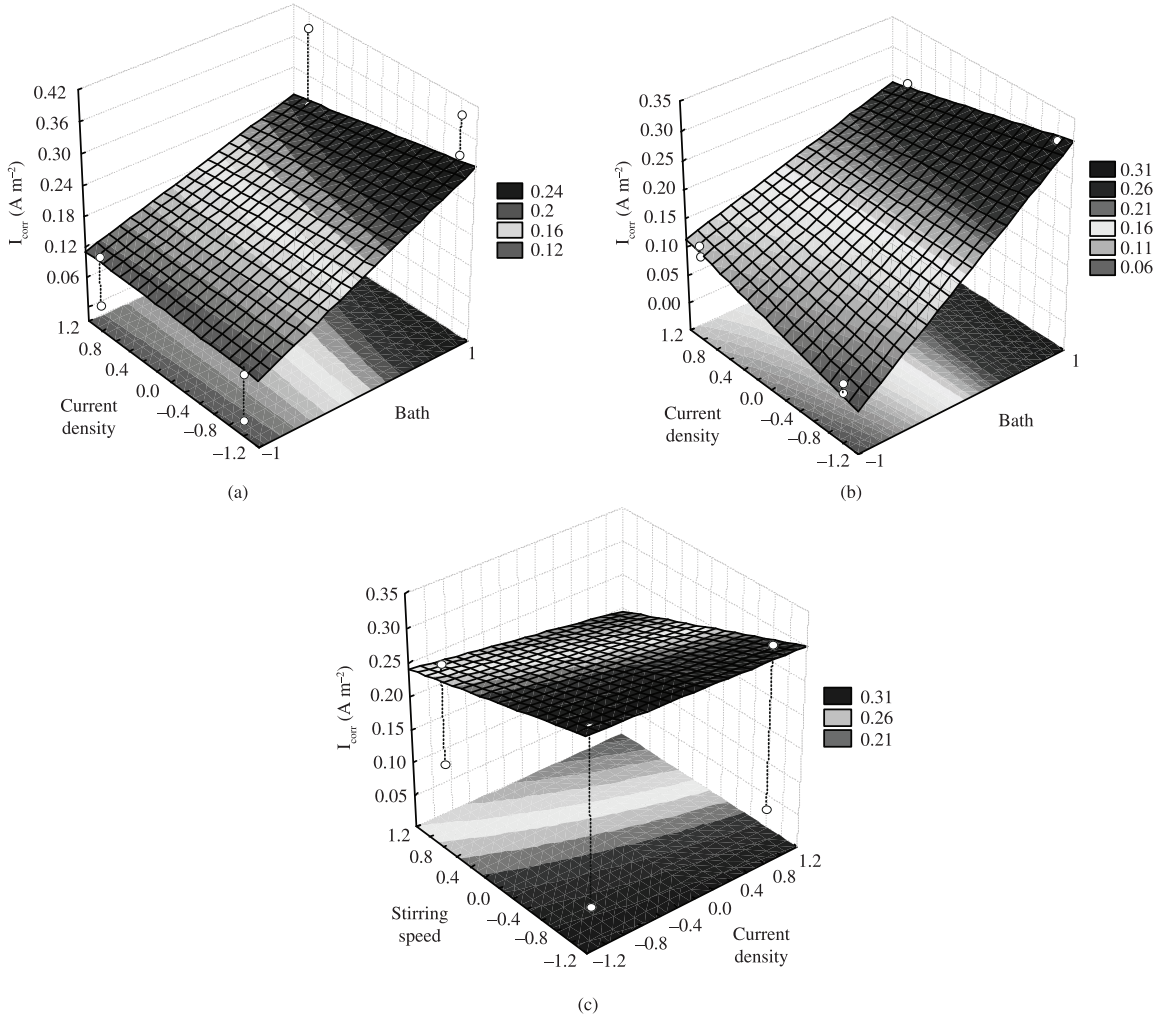

Figure 6. Fitted response surface of standardized effects of a) ***I*** and ***B***; b) ***S*** and ***B*** and c) ***I*** and ***S*** for $\boldsymbol{I_{corr}}$: Bath 2.

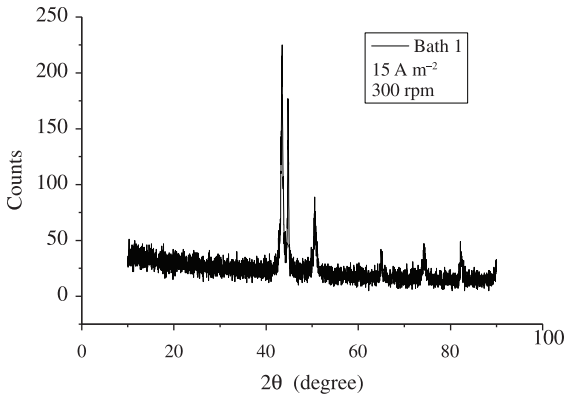

Figure 7. X-rays diffraction of the Cu-Zn coatings produced at 300 rpm and 15 A m^{-2} from Bath 1 of Table 1.

experiment and its polarization curve is also shown. It is interesting to note that the coating/substrate system produced from Bath 3 presents E_{corr} value more positive than the uncoated substrate (–0.38 V_{SCE} and –0.55 V_{SCE} for the coated and the uncoated substrate, respectively), while the E_{corr} for the coating/substrate systems produced from Baths 1 and 2 are at more negative values than the steel (–0.58 V_{SCE} and –0.75 V_{SCE}, for Baths 1 and 2, respectively). The coatings produced from Baths 1 and 3 present only active dissolution in their anodic branches, while a small passivation region is shown in the coating obtained from Bath 2. Only for Bath 3 the cathodic reaction observed seemed to be the oxygen reduction, controlled by mass transport (diffusion), and identified by a bending in the cathodic Tafel curve at approximately –0.60 V_{SCE}.

The $\boldsymbol{I_{corr}}$ values for the substrate/coating systems are shown in Table 3, as well as the $\boldsymbol{I_{corr}}$ value for the uncoated steel substrate is presented (0.30 A m^{-2}), as comparison. The coatings produced from Bath 2 always presented the highest $\boldsymbol{I_{corr}}$ values, regardless of the conditions used, while the lowest values were obtained for the coatings produced from Bath 1. There is a strong, positive, and statistically significant influence of parameter ***B*** (the kind of bath used) in the comparison of Baths 1 and 2, while no statistical effect of the deposition parameters could be noted in the comparison between Baths 1 and 3. This result indicates

that the coatings produced from baths containing cysteine would probably show poorer anticorrosive performance in an aggressive medium. This result is shown in Equation 7, and the adjusted R^2 was found to be approximately 96% in this case. The presence of allyl alcohol in the bath, however, may not have significantly affected the anticorrosive features of the Cu-Zn coatings produced from the citrate bath.

$$\%\hat{I}_{corr} = 0.17 + 0.09B \quad (7)$$

Figure 6 shows the response surfaces relevant to the effects of the studied deposition parameters on $\boldsymbol{I}_{corr}$ of the coatings produced from the bath containing cysteine. In agreement with Equation 7, the bath effect can be easily noted (as shown in Figures 6a, b), regardless of the ***I*** and ***S*** values studied. However, $\boldsymbol{I}_{corr}$ trends (non statistically) to increase at low values of both ***I*** and ***S*** (Figure 6c). These conditions are the same as those used to grow coatings with high copper contents from Bath 2 (Figure 3a), indicating that this kind of coating may not protect the substrate efficiently.

3.5.2. *Coating microstructure and morphology*

Figure 7 presents a diffractogram of the coatings produced from Bath 1 (Table 1) at 300 rpm as an example

Table 4. *d* (*h k l*) values for the Cu-Zn coatings produced from the baths of Table 1.

Observed 2θ	Observed *d* (*h k l*)	*d* (*h k l*) Carbon steel AISI 1020	*d* (*h k l*) Cu (cubic)	*d* (*h k l*) Cu_5Zn_8 (cubic)
43.40	2.086		2.088	2.088
44.76	2.023	2.027		
50.54	1.804		1.808	1.808
65.04	1.433	1.433		
74.25	1.276		1.278	1.279
82.16	1.172	1.170		

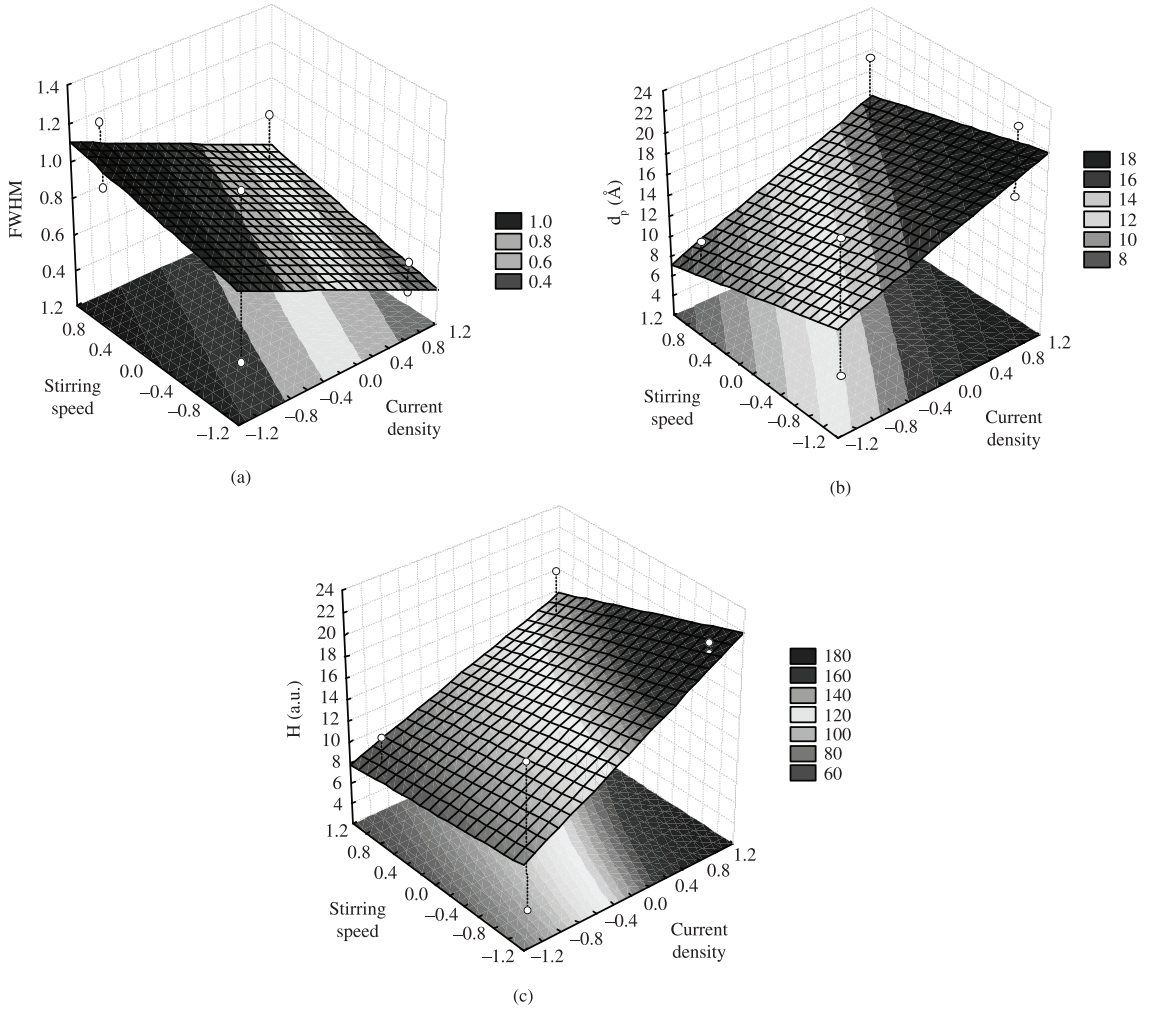

Figure 8. Fitted response surface of standardized effects of ***I*** and ***S*** on: a) ***FWHM***; b) $\boldsymbol{d}_p$ and c) ***H***: Bath 2.

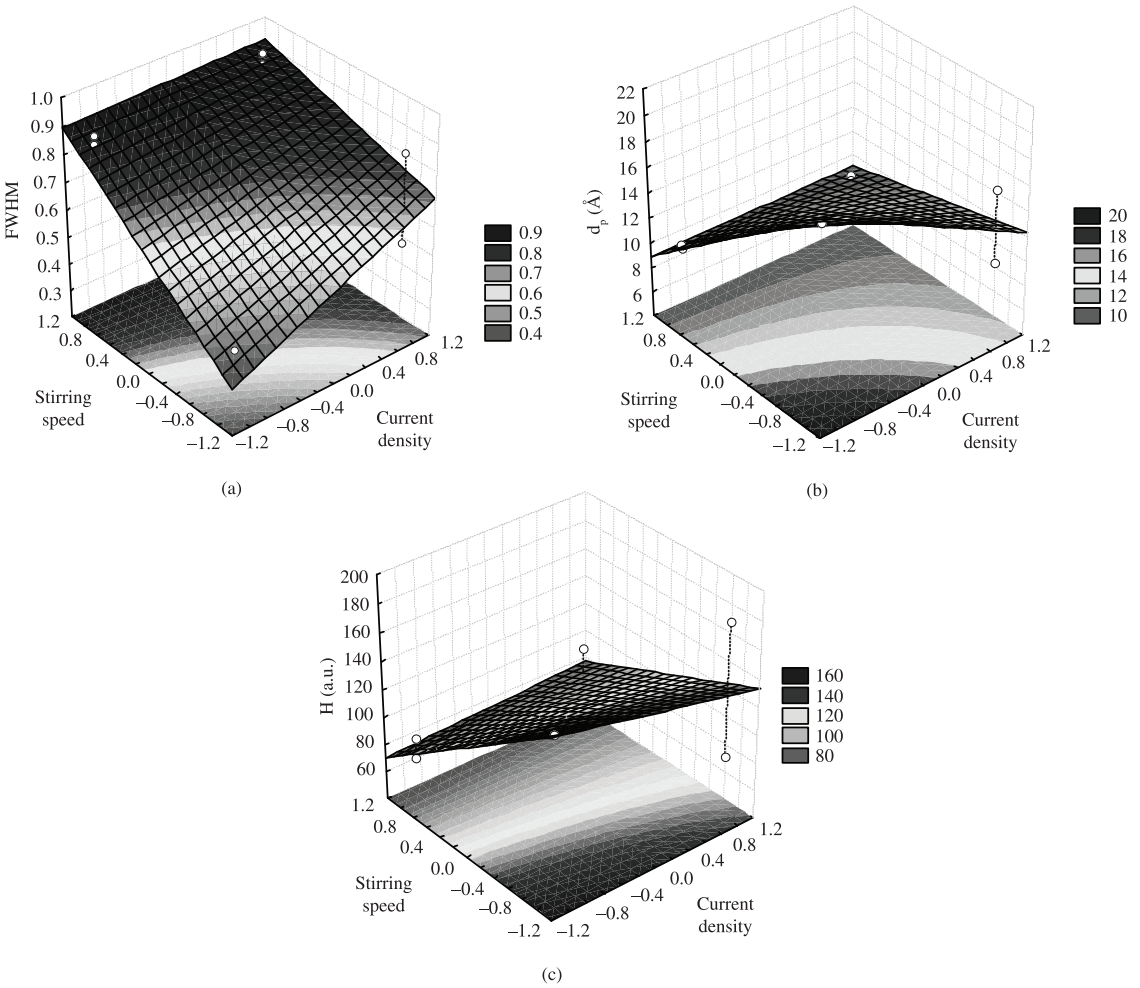

Figure 9. Fitted response surface of standardized effects of ***I*** and ***S*** on: a) ***FWHM***; b) d_p and c) ***H***: Bath 3.

of the coating microstructure. The same diffraction lines are present in all of the diffractograms, regardless of the conditions used to produce the coatings. Most of the peaks are sharp and well defined, indicating that crystalline coatings were obtained. It is possible to see the diffraction lines of the substrate (Fe), as well as those corresponding to the Cu and Cu_5Zn_8 phases (datasheets no. 04-0836, 06-0696, and 25-1228, for the Cu, Fe, and Cu_5Zn_8 phases, respectively)[18]. The crystallographic parameters of the marked diffraction lines are presented in Table 4. The coatings produced from Bath 3 presented microstructures similar to those observed for Bath 1, although the coatings from Bath 3 were always shiny and red-yellowish, while those obtained from Bath 1 were always reddish.

None of the studied deposition parameters exhibited statistically significant influence on the variables ***FWHM***, d_p, or ***H*** of the more intense diffraction line under the conditions employed in this work, although the adjusted R^2 values were always higher than 83% for all responses. There are also some trends that can be observed concerning the effects of ***I*** and ***A*** on these variables for the baths containing additives, as observed in Figures 8 and 9 for Baths 2 and 3, respectively. Additionally, the morphological images of the coatings are presented in Figure 10 for comparison.

For Bath 2, higher values of ***I*** and lower values of ***S*** indicated a decrease in the ***FWHM*** (Figure 8a), with a parallel increase in d_p (Figure 8b) and in ***H*** (Figure 8c), which could be related to an increase in the crystalline characteristics of the coatings. In Figure 10 (experiments 5A to 8A) ***I*** seems to have a greater effect on the increase of G_S. Senna et al.[14] have shown a similar result concerning the effect of ***I*** on the production of Cu-Zn alloys from pyrophosphate baths containing saccharine or butyl alcohol as additives. This effect was related to an increase of the ***% m/m Zn*** in the coatings at higher values of ***I***, which could also increase the residual stress and the microhardness of the coatings[2,3,14]. Although no significant influence of ***I*** on the value of ***% m/m Zn*** was observed for the coatings produced from Bath 2 in the present work, this influence can still provide a possible explanation for the obtained results. Additionally, it is possible to observe cracks on the surfaces of the coatings produced from this bath, which could be correlated to the influence of cysteine on the decrease of the anticorrosive protection, as shown in Equation 7.

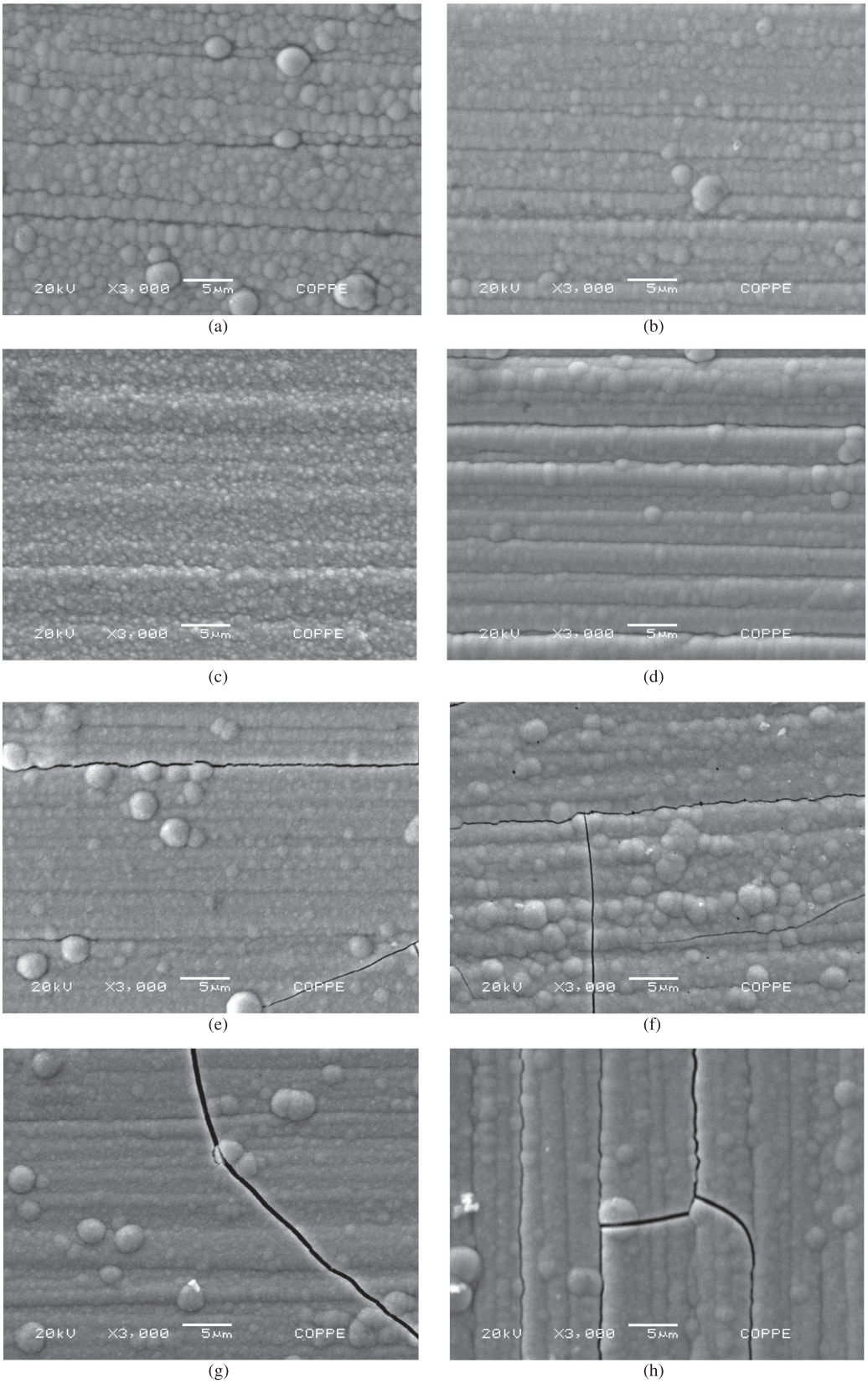

Figure 10. Surface micrographies of the coatings produced from: (a) - (d) Bath 1 (experiments 1 to 4), (e) - (h) Bath 2 (experiments 5A to 8A), (i) - (l) Bath 3 (experiments 5B to 8B) of Table 1.

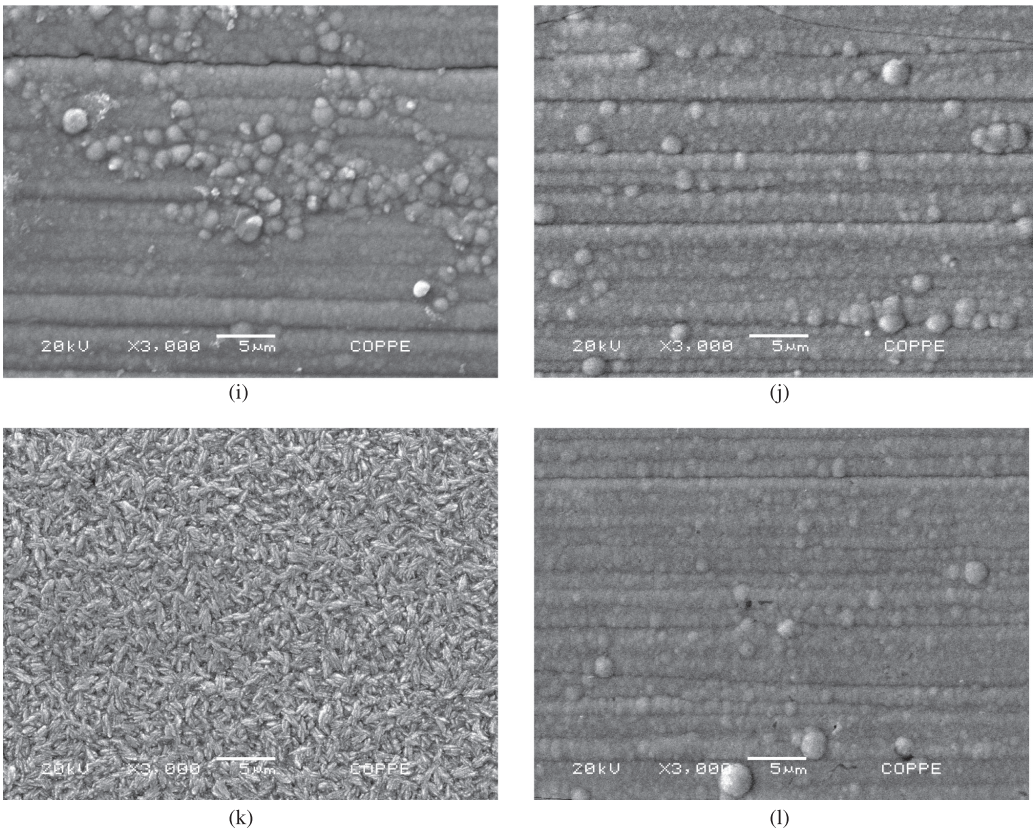

Figure 10. Continuation...

On the other hand, Figure 8 indicates a trend towards smaller d_p values (Figure 8b) at high S values, which is particularly evident at high values of I. This trend is confirmed in Figure 10, in which d_p seems to decrease for high values of I for the samples obtained at 300 and 400 rpm (experiments 6B and 8B). However, this behavior was not observed for samples produced at low I values. Moreover, Equation 6 shows that an increase in $\%\ m/m\ Zn$ was obtained at higher I values for Bath 3, so that an increase in the d_p values would be expected for this condition. It is important to note that most of these results were not statistically significant, and only trends are presented. The effects of the additives themselves could not be completely evaluated, and more experiments are needed to obtain a better conclusion to this inquiry.

4. Conclusions

Cysteine and allyl alcohol were used as additives for Cu-Zn alloys electrodeposited from citrate baths, producing coatings that varied from reddish (for the bath with cysteine) to yellowish (for the bath with allyl alcohol). The presence of cysteine in the bath did not affect the coating composition, although it presented a significant influence on the value of I_{corr}, producing coatings with lower anticorrosive protection in comparison to those produced from Bath 1 (without additives). This result was related to the great amount of cracks observed on the surfaces of these coatings.

The addition of allyl alcohol had no significant effect on the chemical composition of the coatings. Although the coatings obtained from Bath 3 presented an anticorrosive performance similar to those produced from the bath without additives, they exhibited higher shine and had a chemical composition near that of commercial brass. Their surfaces presented a small grain size, with no cracks or pores. This behavior can be attributed to the surfactant effect of allyl alcohol in the solutions.

Acknowledgements

The authors would like to thank the Rio de Janeiro Research Foundation (FAPERJ), the Brazilian National Research Council (CNPq), and the State University of Rio de Janeiro (UERJ) for financial support. We would also like to thank D.Sc. Deborah Vargas for helping in the X-rays analysis.

References

1. Díaz SL. *Eletrodeposição de ligas Cu/Zn*. Rio de Janeiro: Federal University of Rio de Janeiro; 1988. (COPPETEC Project No. PP-3414).
2. Senna LF. *Estudo de parâmetros para eletrodeposição de ligas Cu/Zn em eletrólitos de pirofosfato*. [Dissertation]. Rio de Janeiro: Federal University of Rio de Janeiro; 1991.
3. Vagramyan TA. Electrodeposition of Alloys. In: Kruglikov SS, editor. *Electrochemistry*. Jerusalem: Israel Program of Scientific Translation Ltd.; 1970. p. 1-129.
4. Lainer VI. *Modern electroplating*. Jerusalem: Israel Program of Scientific Translation Ltd; 1970.
5. Oniciu L and Muresan L. Some fundamental aspects of leveling and brightening in metal electrodeposition. *Journal of Applied Electrochemistry.* 1991; 21(7):565-574. http://dx.doi.org/10.1007/BF01024843
6. Marti EM, Methivier C and Pradier CM. (*S*)-Cysteine Chemisorption on Cu(110), from the Gas or Liquid Phase: An FT-RAIRS and XPS Study. *Langmuir.* 2004; 20(23):10223-10230. http://dx.doi.org/10.1021/la048952w
7. Mohamed AE, Rashwan SM, Abdel-Wahaab SM and Kamel MM. Electrodeposition of Co-Cu alloy coatings from glycinate baths. *Journal of Applied Electrochemistry*. 2003; 33(11):1085-1092. http://dx.doi.org/10.1023/A:1026209715687
8. Matos JB, Pereira LP, Agostinho SML, Barcia OE, Cordeiro GGO and D'Elia E. Effect of cysteine on the anodic dissolution of copper in sulfuric acid medium. *Journal of Electroanalytical Chemistry.* 2004; 570(1):91-94. http://dx.doi.org/10.1016/j.jelechem.2004.03.020
9. Ihs A and Lieberg B. Chemisorption of L-cysteine and 3-mercaptopropionic acid on gold and copper surfaces - an infrared reflection absorption study. *Journal Of Colloid and Interface Science.* 1991; 144(1):282-292. http://dx.doi.org/10.1016/0021-9797(91)90259-B
10. Sigel H, editor. *Metal ions in biological systems*: amino acids and derivatives as ambivalent ligands. New York: Marcel Dekker, Inc.; 1979. v. 9.
11. Vargalyuk VF, Loshkarev YM, Polonskii VA and Khoroshavkina NV. Kinetics and mechanism of copper(II) in the presence of certain unsatured organic compounds - Allyl alcohol. *Soviet Electrochemistry*. 1986; 22(9):1229-1231.
12. Naohisa Y, Ogura T, Scott N and Fernando Q. Kinetics of the Reduction of Copper (II) to Copper (I) in aqueous Solutions and the Complexation of the Copper(I) with Allyl Alcohol. *Analytical Chemistry.* 1984; 56(14):2830-2834. http://dx.doi.org/10.1021/ac00278a045
13. Senna LF, Díaz SL and Sathler L. Electrodeposition of copper-zinc alloys in pyrophosphate-based electrolytes. *Journal of Applied Electrochemistry.* 2003; 33(12):1155-1161. http://dx.doi.org/10.1023/B:JACH.0000003756.11862.6e
14. Senna LF, Díaz SL. and Sathler L. Hardness analysis and morphological characterization of copper-zinc alloys produced in pyrophosphate-based electrolytes. *Materials Research*. 2005; 8(3):275-279. http://dx.doi.org/10.1590/S1516-14392005000300009
15. Medvedev GI and Makrushin NA. Electrodeposition of Tin from Sulfate Electrolyte in the Presence of Syntanol, Formaldehyde, and Allyl Alcohol. *Russian Journal of Applied Chemistry.* 2004; 77(11):1781-1785. http://dx.doi.org/10.1007/s11167-005-0159-5
16. Ferreira FBA, Silva FLG, Luna AS, Lago DCB and Senna LF. Response surface modeling and optimization to study the influence of deposition parameters on the electrodeposition of Cu-Zn alloys in citrate medium. *Journal of Applied Electrochemistry*. 2007; 37(4):473-481. http://dx.doi.org/10.1007/s10800-006-9278-9
17. Silva FLG, Lago DCB, D'Elia E. and Senna LF. Electrodeposition of Cu-Zn alloy coatings from citrate baths containing benzotriazole and cysteine as additives. *Journal of Applied Electrochemistry*. 2010; 40(11):2013-2022. http://dx.doi.org/10.1007/s10800-010-0181-z
18. Joint Committee on Powder Diffraction Standards - JCPDS. *Powder Diffraction File - PDF-2*. Pennsylvania: ICDD; 2000. CD-ROM.
19. Cullity BD. *Elements of X-rays diffraction.* 2nd ed. London: Addison-Wesley Publishing Company, Inc.; 1978.
20. Silva FLG, Garcia JR, Cruz VGM, Luna AS, Lago DCB and Senna LF. Response surface analysis to evaluate the influence of deposition parameters on the electrodeposition of Cu-co alloys in citrate medium. *Journal of Applied Electrochemistry*. 2008; 38(12):1763-1769. http://dx.doi.org/10.1007/s10800-008-9630-3
21. Senna LF, Luna AS. Experimental design and response surface analysis as available tools for statistical modelling and optimization of electrodeposition processes. In: Sebayang D and Hasan SBH. *Electroplating*. In Tech Open Access Edition. Rijeka; 2012.
22. Chassaing E, Quang KV and Wiart R. Kinetics of copper electrodeposition in citrate electrolytes. *Journal of Applied Electrochemistry*. 1986; 16(4):591-604. http://dx.doi.org/10.1007/BF01006854
23. Rode S, Henninot C, Vallières C and Matlosz M. Complexation Chemistry in Copper Plating from Citrate Baths. *Journal of the Electrochemical Society.* 2004; 151(6):C405-C411. http://dx.doi.org/10.1149/1.1715092
24. Sukava AJ, Schneide H, McKenney DJ and McGregor AT. Cathode overpotential and surface-active additives in electrodeposition of copper. II. Effects of compounds containing divalent sulfur. *Journal of the Electrochemical Society*. 1965; 112(6):571-573. http://dx.doi.org/10.1149/1.2423608
25. Lurie J. *Handbook Analytical Chemistry*. Moscou: Mir Publishers; 1978.
26. Gockel P, Vahrenkamp H and Zuberbuhler AD. Zinc-complexes of cysteine, histidine, and derivatives thereof - potentiometric determination of their compositions and stabilities. *Helvetica Chimica Acta*. 1993; 76(1):511-520. http://dx.doi.org/10.1002/hlca.19930760133